

# Metall-Substrat-Wechselwirkungen in der heterogenen Katalyse: Vertiefte Einblicke in die atomare Struktur von Grenzflächen durch höchstauflösende Mikroskopie an Modell Systemen \*\*

M.G. Willinger\*, W. Zhang, O. Bondarchuk, S. Shaikhutdinov\*, H.-J. Freund, R. Schlögl

**Abstract.** Die Symbiose aus hochauflösender Rastersonden- und Elektronenmikroskopie mit wohl definierten Modell Systemen ermöglicht einen Detaillierten Einblick in die Beschaffenheit relevanter Grenzflächen in nano-strukturierten katalytischen Systemen. Dies wird hier anhand von Pt Nanopartikeln auf einem Eisenoxid Träger demonstriert, welche aufgrund einer starken Wechselwirkung zwischen Metall und Substrat von einer dünnen Oxidschicht benetzt werden.

Ein erfolgreicher Ansatz für die gezielte Modifikation katalytischer Eigenschaften von metallischen Nanopartikeln besteht in der Wahl eines geeigneten Substrats. In der Tat gibt es eine ganze Klasse von „nicht inerten“ Trägern, bei denen eine entsprechender Präparation zur Ausbildung einer starken Metall-Substrat-Wechselwirkung („strong metal/support interaction“, SMSI) mit den aufgebracht Metal Partikeln führt.<sup>[1]</sup> Unter anderem kann es dadurch zur Ausbildung von Hetero-Grenzflächen zwischen den Metal Partikeln und einer halbleitenden (oxidischen) dünnen Schicht kommen, welche die elektronische Struktur und dadurch die adsorptions-Eigenschaften des Systems verändert.<sup>[2]</sup> Die Benetzung der Metal Partikel durch ein Oxid führt in der Regel zur Unterdrückung der katalytischen Aktivität. In bestimmten Fällen und in Abhängigkeit des chemischen Potentials der Gas-Phase, kann es jedoch auch zur Ausbildung einer erhöhten Reaktivität und herausragender Selektivität führen.<sup>[3]</sup> Obgleich die phänomenologischen Effekte wohl bekannt sind und ausgenutzt werden, fehlt das zugrundeliegende Verständnis des SMSI-Zustandes auf atomarem Niveau. Im Speziellen benötigt die Theorie eine exakte Beschreibung des SMSI Zustandes für die Vorhersage ihrer Funktion.

Mit der Verfügbarkeit von aberrations korrigierten Linsen für Transmissionselektronenmikroskope (TEM)<sup>[4]</sup> haben sich neue Möglichkeiten für die Untersuchung der Struktur von Katalysatoren eröffnet. Im speziellen betrifft das die atomar aufgelöste Abbildung von Oberflächen,<sup>[5]</sup> was zuvor nur mittels Rastertunnelmikroskopie

(STM) an planaren Modellsystemen erreicht werden konnte.<sup>[6]</sup>

Zur Bereitstellung eines eperimentellen Fundaments für ein atomares Verständnis des SMSI Zustandes wurde ein Model System, bestehend aus Pt Nanopartikeln auf einer wohlgeordneten Fe<sub>3</sub>O<sub>4</sub>(111) Schicht, mittels hochauflösender Elektronenmikroskopie (STM und TEM) untersucht. In einer vorangehenden Studie konnte mittels STM gezeigt werden, daß Heizen im ultrahoch-Vakuum zu einer Benetzung der Pt Partikel mit einer dünnen Schicht, die einer monolage von FeO(111) entspricht, führt<sup>[6b, 7]</sup> (Abbildungen 1a,b). Ergänzende Studien zur Reaktivität unter Atmosphärendruck zeigten eine erhöhte Aktivität in der CO oxidation im Vergleich zu reinen Pt Partikeln.<sup>[3d]</sup> Weitere Untersuchungen<sup>[8]</sup> zeigten, daß eine auf Pt(111) Einkristallen aufgewachsene Monolage von FeO(111) eine viel höhere Aktivität zeigt als reines Pt(111) beziehungsweise als mehrere nanometer dicke Fe<sub>3</sub>O<sub>4</sub>(111) Filme, was ein weiteres Indiz dafür ist, daß die erhöhte Reaktivität direkt mit der atomaren Struktur der ultra-dünnen Eisenoxid-Schicht auf dem Pt zusammenhängt. Eine Bestätigung der STM Daten druch eine direkte Messung der chemischen Komposition stand bisher aus. Ausserdem bestehen offene Fragen bezüglich der Struktur der Grenzflächen zwischen den Pt Partikeln und der einhüllenden oxid-Schicht auf der einen, sowie zum Fe<sub>3</sub>O<sub>4</sub>(111) Substrat auf der anderen Seite. Schlußendlich ist auch der zugrundeliegende Mechanismus für die Benetzung bisher nicht aufgeklärt.

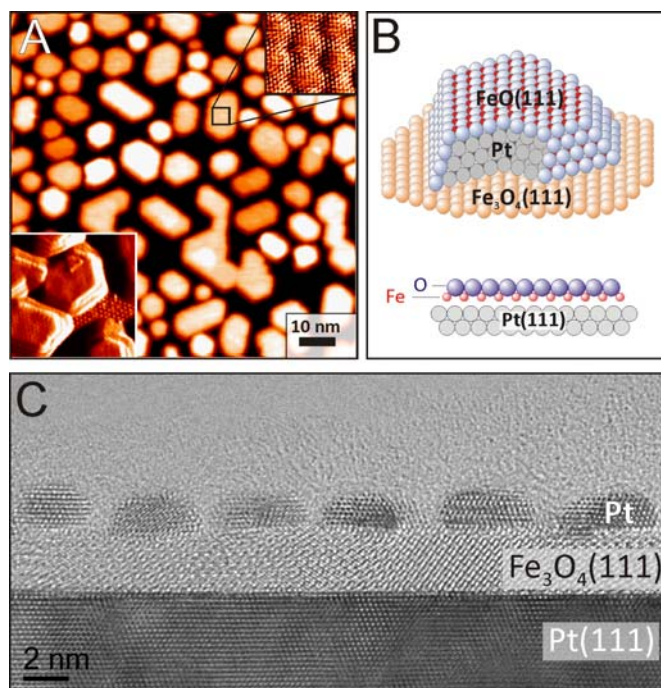


Abbildung 1. (A) Representative STM Aufnahme einer Pt/Fe<sub>3</sub>O<sub>4</sub>(111) Oberfläche nach thermischer Behandlung im UHV bei 850 K. (B) Schematische Darstellung eines benetzten Pt Partikels und einer Grenzschicht zwischen einer Monolage von FeO(111) auf Pt(111). (C) TEM Aufnahme des Pt/Fe<sub>3</sub>O<sub>4</sub>(111) Systems im Querschnitt.

[\*] Dr. M.G. Willinger, Dr. W. Zhang, Dr. O. Bondarchuk, Dr. S. Shaikhutdinov, Prof. Dr. H.-J. Freund, Prof. Dr. R. Schlögl  
Fritz Haber Institute of the Max Planck Society  
Faradayweg 4-6, 14195 Berlin (Germany)  
Fax: (+49) 30-8413-4105  
Email: shaikhutdinov@fhi-berlin.mpg.de;  
willinger@fhi-berlin.mpg.de

[\*\*] This work has been supported by the Deutsche Forschungsgemeinschaft. The authors wish to recognize Dr. Yu. Martynova (FHI) and Mr. Yasuhara (JEOL Ltd) for technical assistance.

Abbildung 1c zeigt eine typische hochauflösende TEM (HRTEM) Aufnahme des untersuchten Pt/Fe<sub>3</sub>O<sub>4</sub>(111) Systems im Querschnitt, welches die epitaktischen Beziehungen zwischen einem Pt(111) Träger, einer Fe<sub>3</sub>O<sub>4</sub>(111) Schicht und den Pt Partikeln erkennen läßt (siehe auch Hintergrundinformationen, Abbildung S1). In Morphologie und Größe stimmen die Partikel mit den STM Beobachtungen überein. Um einen Einblick in die atomare Struktur der Grenzschichten zu erhalten, wurde die Probe im Raster Modus mittels eines Detektors im Bereich hoher Streuwinkel (HAADF STEM) untersucht (siehe Abbildung 2).

Zuerst richten wir die Aufmerksamkeit auf die Grenzfläche zwischen dem Pt(111) Träger und dem Fe<sub>3</sub>O<sub>4</sub>(111) Substrat. In Abbildung 2a zeigt die Anordnung atomarer Säulen wie sie in Transmission zu sehen ist. Es ist zu erkennen daß die erste Schicht atomarer Säulen oberhalb der sehr hellen Pt Säulen eine etwas geringfügigere Intensität aufweist.

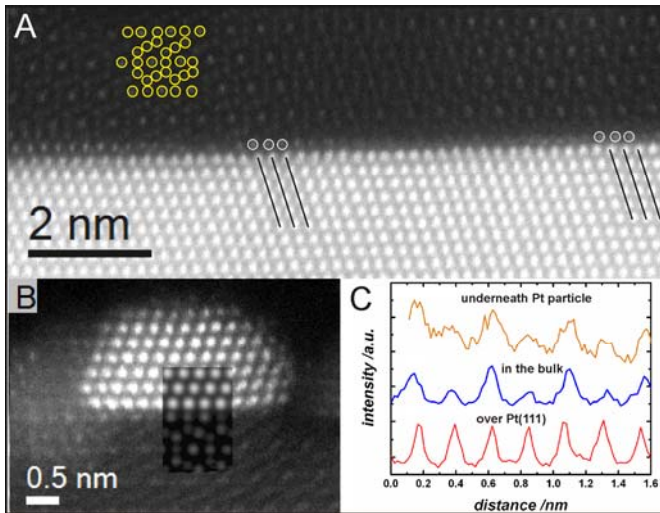


Figure 2. HAADF STEM images of interfaces between: a Pt(111) substrate and an Fe<sub>3</sub>O<sub>4</sub>(111) film (A); an oxide film and a supported Pt particle (B). The Fe atomic columns in the Fe<sub>3</sub>O<sub>4</sub>(111) bulk are marked by circles. Registry variations of the interfacial oxide layer with respect to the Pt(111) surface are highlighted. (C) Intensity profiles measured for the atomic columns in the first oxide layer over a Pt(111) substrate (top), and underneath the Pt particle shown in image B (bottom). The intensity profile along the Kagomé layer in the bulk of the Fe<sub>3</sub>O<sub>4</sub>(111) film is shown for comparison.

Ausserdem zeichnet sich diese Schicht durch einen etwas vergrößerten Gitter-Abstand im Vergleich zur darunterliegenden Pt Schicht aus. Diese Abweichung in der Periodizität für zur beobachtbaren Modulation des Kontrastes entlang der Schnittstelle. Diese Schicht kann daher dem Eisenoxid zugeordnet werden. Es empfiehlt sich an dieser Stelle, sich die Festkörper Struktur von Fe<sub>3</sub>O<sub>4</sub>(111) in Erinnerung zu rufen. Sie zeichnet sich (auch Hintergrundinformationen, Abbildung S2) may be viewed as closed-packed monolayers (ML) of oxygen ions with a 2.97 Å lattice constant separated by two different iron layers which alternate in stacking order.<sup>[9]</sup> One is a mix-trigonal layer that in turn consists of three Fe layers ¼ ML each (totally ¾ ML); and the second one is a so-called Kagomé layer (¾ ML).

As a starting point to a structural analysis, we employed the model, previously proposed by Roddatis et al.<sup>[10]</sup> on the basis of high resolution TEM images, in which the Kagomé layer is placed over Pt(111). However, the intensity of the Fe columns in a Kagomé layer has to alternate according to the density of the Fe atoms along the columns (in 2:1 ratio, see Fig. S2). This is clearly observed in the film bulk (see line profiles in Fig. 2c), but it is definitely not the

case for the interfacial layer. The adjacent columns exhibit near equal intensity, thus suggesting that the interfacial layer, in fact, consists of a close-packed Fe layer like in FeO(111). The interlayer distance measured between the Fe and Pt columns (2 Å, on average) is too small for having any O-layer (hardly visible in TEM) in between. Bearing in mind that a FeO(111) monolayer on Pt(111) is stacked as O-Fe-Pt (Fig. 1b), and this layer is first prepared on Pt(111) prior to a subsequent layer-by-layer growth of the Fe<sub>3</sub>O<sub>4</sub>(111) film, we conclude that the film/substrate interface consists of a close-packed Fe-layer over Pt(111).

Applying the same approach to the interface between a Pt particle and a Fe<sub>3</sub>O<sub>4</sub>(111) film, we found that it consists of a Kagomé layer exposed to the Pt(111) facet of the particle as shown in Fig. 2b. Indeed, this interfacial layer exhibits the above-mentioned intensity oscillation (Fig. 2c). Again, the interlayer distance between the Pt and Fe columns (~ 2 Å) indicates the absence of an O-layer in between.

The difference between the two interfaces (Pt(111)/Fe<sub>3</sub>O<sub>4</sub>(111) vs Fe<sub>3</sub>O<sub>4</sub>(111)/Pt(111)) may, in first approximation, be explained by the preparation: The film growth involved annealing in 10<sup>-6</sup> mbar O<sub>2</sub> at ~ 1000 K, whereas the Pt particles were heated in UHV to 850 K only. More intriguing is the finding that a Pt particle sits on top of the Kagomé layer, which is not the most stable termination of a pristine Fe<sub>3</sub>O<sub>4</sub>(111) film. It has previously been shown, that the Fe<sub>3</sub>O<sub>4</sub>(111) surface is represented by a ¼ ML Fe in a (2x2) structure over the O-layer (Fig. S1),<sup>[9]</sup> although some small ill-defined clusters may be present at the film surface.<sup>[11]</sup> Therefore, upon Pt deposition, particle growth and subsequent high-temperature annealing, the surface Fe and O layers are removed for the Pt(111) layer in the particle to bind the Kagomé layer, which is the next Fe-containing layer below the topmost Fe-layer in the pristine film. It, therefore, appears that the interface between Pt(111) and Fe<sub>3</sub>O<sub>4</sub>(111) is formed in such a way, that it maximizes the number of Pt/Fe bonds. Indeed, the amount of Fe in the Kagomé layer is 3 times higher than in the terminating Fe-layer. The preferential formation of the Pt-Fe bonds at the interface may also be traced back from simplified metal/oxide junction considerations. The work function of Fe<sub>3</sub>O<sub>4</sub>(111) (~ 5.5 eV) is lower than of Pt(111) (= 5.93 eV), therefore the contact between Pt and iron oxide would result in electron transfer from oxide to Pt, which will drive the positively charged Fe ions to be at the interface.<sup>[12]</sup>

Now we address the surface structure of the supported Pt particles studied by HRTEM. Figure 3a clearly shows that the particle surface exhibits a low-contrast, uniform atomic layer with the periodicity of atomic columns obviously larger than that of underlying Pt(111). This finding is fully consistent with the STM results, suggesting the formation of an FeO(111) layer having a larger lattice constant (~ 3.05 Å) than Pt(111) (= 2.78 Å). Using the distance between the Pt columns in Pt(111) as an internal reference (= 2.4 Å), the measured distance between the columns in the surface overlayer (~ 2.7 Å) agrees well with 2.62 Å expected for the Fe columns in the FeO(111) monolayer.

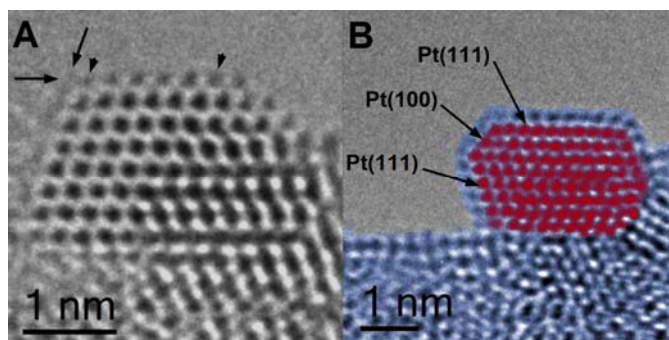


Figure 3. HRTEM images of Pt particles supported by  $\text{Fe}_3\text{O}_4(111)$  in the SMSI state. (A) The long arrows indicate the encapsulated layer, the short arrows highlight the relative displacement of the topmost row of atoms with respect to the Pt atoms underneath. (B) Colorized image to illustrate continuous encapsulation layer on different facets of a Pt particle as indicated. (The original images are shown in Fig. S3).

Furthermore, the HRTEM images show that the side facets, which could not be resolved by STM, are covered essentially by the same oxide layer (Figs. 3b, S3). Although this has been proposed on the basis of CO adsorption experiments<sup>[7]</sup> and previous STM studies of  $\text{FeO}(111)$  films on a  $\text{Pt}(100)$  substrate,<sup>[13]</sup> the HRTEM images provide direct evidence for the encapsulation of the whole Pt particle by the  $\text{FeO}(111)$  layer.

The chemical composition of the surface layer was examined by electron energy loss spectroscopy (EELS) in the STEM mode having certain advantage over conventionally used energy dispersive x-ray spectroscopy.<sup>[14]</sup> Figure 4 displays the EELS spectrum, obtained from interior regions of the  $\text{Fe}_3\text{O}_4(111)$  film, showing the K-edge of O and the L-edge of Fe approximately at 530 eV and 710 eV, respectively. Basically the same features with a much lower intensity are observed in the EELS spectrum at the surface of the imaged Pt particle, thus suggesting that the encapsulated layer seen by HRTEM (Fig. 3) and STM (Fig. 1a) contains both oxygen and iron, although its stoichiometry cannot be determined precisely.

Notably, the interlayer distance (2.3 Å) measured by HRTEM between the Pt and Fe columns in Fig. 3 is considerably larger than 2 Å measured between those at the  $\text{Pt}(111)/\text{Fe}_3\text{O}_4(111)$  interface (Fig. 2), and 1.3 Å previously obtained for a  $\text{FeO}(111)$  monolayer film on  $\text{Pt}(111)$ ,<sup>[15]</sup> both structures having the Pt-Fe bonds. Our recent studies have shown that the  $\text{FeO}(111)$  monolayer readily transforms into the O-Fe-O trilayer structure at oxygen pressures above  $10^{-2}$  mbar.<sup>[8a]</sup> Accordingly, the distance between the Fe and Pt layers increases from 1.3 Å to approximately 2.2 Å. Although the investigated sample has been passivated in UHV with a relatively thick amorphous carbon film, it appears that the original  $\text{FeO}$  film encapsulating Pt particles transforms here into the O-Fe-O trilayer upon adventitious reaction with air during the sample preparation (see Supporting Information). The observed interlayer distance (2.3 Å) agrees well with the O-Fe-O-Pt(111) structure of the encapsulated film imaged in Fig. 3.

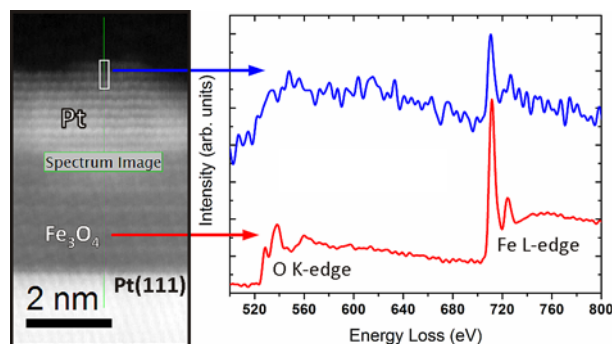


Figure 4. EELS spectra (after baseline subtraction) taken along the line scan as indicated.

Finally, we address the source of the iron oxide encapsulating Pt particles. Clearly, the amount of iron in the topmost layer in the pristine film (i.e.,  $\frac{1}{4}$  ML), which is laterally contracted upon Pt deposition and annealing (see the above discussion), is not sufficient to cover a whole particle with a Fe monolayer. Therefore, there must be another source of iron, ultimately encapsulating the Pt particle upon high-temperature annealing. One could envision basically two scenarios: either Fe from the layer(s) underneath the particle migrates through the particle (virtually via alloying), or Fe migrates onto the Pt surface from the surrounding area. Previously, on the basis of high energy electron diffraction measurements of  $\text{Pd}/\text{TiO}_2(110)$ , it has been concluded that the encapsulating material is transported by surface migration.<sup>[16]</sup> It should be mentioned, however, that  $\text{TiO}_2$  single crystals normally possess extra-Ti atoms, located in interstitial sites in the bulk which readily migrate towards the surface upon heating.<sup>[17]</sup> In contrast, the thin  $\text{Fe}_3\text{O}_4(111)$  films, prepared under well-controlled conditions, are essentially stoichiometric.

Thorough inspection of numerous STEM images revealed substantial contrast variations in the regions surrounding Pt particles as shown in Fig. 5. The annular bright field (ABF) and HAADF STEM images indicated a loss of iron atoms and lack of ordering in those areas. (A similar picture was also observed underneath the particles, but we assign this effect to the uncovered oxide areas in front and/or behind the imaged Pt particle, as the images are recorded in projection). These findings favour the conclusion that the encapsulation proceeds through surface migration of Fe species from the oxide onto the Pt particle surface.

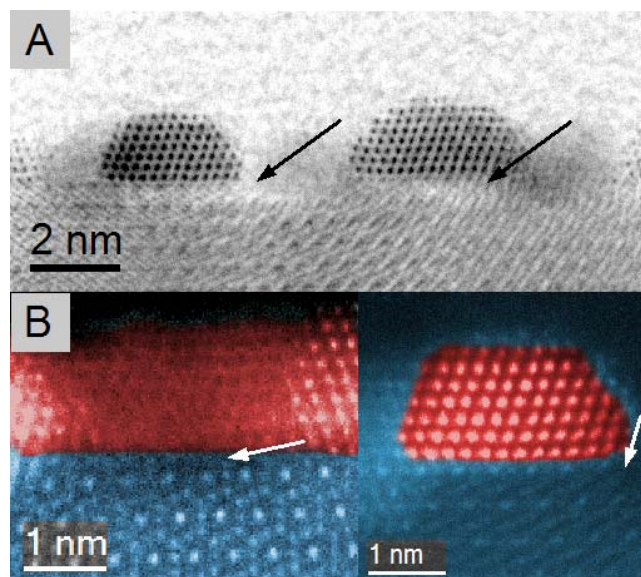


Figure 5. The ABF (a) and colorized HAADF (b) STEM images illustrating a loss of material and a lack of ordering in the oxide support as highlighted by the arrows.

In summary, we show that a symbiosis of advanced methods of scanning probe and electron microscopies and well-defined model systems provides a detailed picture of interfaces in nanostructured catalytic systems. This was demonstrated for Pt nanoparticles supported on a well-ordered iron oxide thin film which undergo encapsulation by supporting oxide in the course of strong metal/support interaction. Furthermore, it is possible to reconstruct the localization of the oxide support material flowing over the metal particle. It appears that charge transfer from a transition metal oxide to highly electronegative Pt maximizes the number of Pt-cation (in this case, Fe) contacts at the interface. Depending on the chemical potential of reacting gases, phase separation into thicker layers of oxide and bare metal particles may become more favourable. The results provide additional information for theory to construct a detailed energetic picture of formation, stability and effect of complex interfaces in catalysis.

Received: ((will be filled in by the editorial staff))  
Published online on ((will be filled in by the editorial staff))

**Keywords:** strong metal-support interaction • model systems • high resolution electron microscopy • ultrathin oxide films

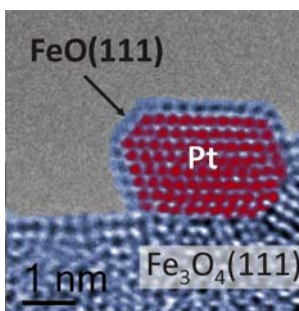
- [1] S. J. Tauster, *Accounts of Chemical Research* **1987**, *20*, 389-394.
- [2] a) F. Solymosi, *Catalysis Reviews* **1968**, *1*, 233-255; b) G. L. Haller, D. E. Resasco, in *Advances in Catalysis, Vol. Volume 36* (Eds.: H. P. D.D. Eley, B. W. Paul), Academic Press, **1989**, pp. 173-235; c) A. A. Slinkin, E. A. Fedorovskaya, *Russian Chemical Reviews* **1971**, *40*, 860; d) G.-M. Schwab, in *Advances in Catalysis, Vol. Volume 27* (Eds.: H. P. D.D. Eley, B. W. Paul), Academic Press, **1979**, pp. 1-22; e) F. F. Vol'kenshtein, *Russian Chemical Reviews* **1966**, *35*, 537; f) H.-J. Freund, G. Pacchioni, *Chemical Society Reviews* **2008**, *37*, 2224-2242; g) Q. Fu, T. Wagner, *Surface Science Reports* **2007**, *62*, 431-498.
- [3] a) E. J. Braunschweig, A. D. Logan, A. K. Datye, D. J. Smith, *Journal of Catalysis* **1989**, *118*, 227-237; b) M. Behrens, F. Studt, I. Kasatkin, S. Kühl, M. Hävecker, F. Abild-Pedersen, S. Zander, F. Girgsdies, P. Kurr, B.-L. Kniep, M. Tovar, R. W. Fischer, J. K. Nørskov, R. Schlögl, *Science* **2012**, *336*, 893-897; c) S. Bernal, J. J. Calving, G. A. Cifredo, J. M. Rodríguez-Izquierdo, V. Perrichon, A. Laachir, *Journal of Catalysis* **1992**, *137*, 1-11; d) M. Lewandowski, Y. N. Sun, Z. H. Qin, S. Shaikhutdinov, H. J. Freund, *Applied Catalysis a-General* **2011**, *391*, 407-410.
- [4] M. Haider, H. Rose, S. Uhlemann, B. Kabius, K. Urban, *Journal of Electron Microscopy* **1998**, *47*, 395-405.
- [5] a) J. Liu, *ChemCatChem* **2011**, *3*, 934-948; b) J. M. Thomas, C. Ducati, R. Leary, P. A. Midgley, *ChemCatChem* **2013**, *5*, 2560-2579; c) W. Zhou, I. E. Wachs, C. J. Kiely, *Current Opinion in Solid State and Materials Science* **2012**, *16*, 10-22.
- [6] a) O. Dulub, W. Hebenstreit, U. Diebold, *Physical Review Letters* **2000**, *84*, 3646-3649; b) Z. H. Qin, M. Lewandowski, Y. N. Sun, S. Shaikhutdinov, H. J. Freund, *The Journal of Physical Chemistry C* **2008**, *112*, 10209-10213.
- [7] Z. H. Qin, M. Lewandowski, Y. N. Sun, S. Shaikhutdinov, H. J. Freund, *J. Phys.-Condes. Matter* **2009**, *21*.
- [8] a) Y.-N. Sun, L. Giordano, J. Goniakowski, M. Lewandowski, Z.-H. Qin, C. Noguera, S. Shaikhutdinov, G. Pacchioni, H.-J. Freund, *Angewandte Chemie-International Edition* **2010**, *49*, 4418-4421; b) Y. N. Sun, Z. H. Qin, M. Lewandowski, E. Carrasco, M. Sterrer, S. Shaikhutdinov, H. J. Freund, *Journal of Catalysis* **2009**, *266*, 359-368.
- [9] M. Ritter, W. Weiss, *Surface Science* **1999**, *432*, 81-94.
- [10] V. V. Roddatis, D. S. Su, C. Kuhrs, W. Ranke, R. Schlögl, *Thin Solid Films* **2001**, *396*, 78-83.
- [11] A. Sala, H. Marchetto, Z. H. Qin, S. Shaikhutdinov, T. Schmidt, H. J. Freund, *Physical Review B* **2012**, *86*, 155430.
- [12] a) J. Goniakowski, C. Noguera, *Physical Review B* **2009**, *79*, 155433; b) J. Goniakowski, C. Noguera, L. Giordano, G. Pacchioni, *Physical Review B* **2009**, *80*, 125403.
- [13] S. Shaikhutdinov, M. Ritter, W. Weiss, *Physical Review B - Condensed Matter and Materials Physics* **2000**, *62*, 7535-7541.
- [14] D. A. Muller, L. F. Kourkoutis, M. Murfitt, J. H. Song, H. Y. Hwang, J. Silcox, N. Dellby, O. L. Krivanek, *Science* **2008**, *319*, 1073-1076.
- [15] Y. J. Kim, C. Westphal, R. X. Ynzunza, H. C. Galloway, M. Salmeron, M. A. Van Hove, C. S. Fadley, *Physical Review B* **1997**, *55*, R13448-R13451.
- [16] T. Suzuki, R. Souda, *Surface Science* **2000**, *448*, 33-39.
- [17] M. Bowker, P. Stone, P. Morrall, R. Smith, R. Bennett, N. Perkins, R. Kvon, C. Pang, E. Fourre, M. Hall, *Journal of Catalysis* **2005**, *234*, 172-181.

## Interface in Catalysis

M. Willinger\*, W. Zhang,  
O. Bondarchuk, S.  
Shaikhutdinov\*, H.-J.  
Freund, R. Schlögl

Page –  
Page

Combining the Advanced  
Microscopies and Model  
Systems to Elucidate the  
Atomic Structure of  
Interface: A Case of  
Metal/Support Interaction



A symbiosis of advanced scanning probe and electron microscopies and a well-defined model system may provide a detailed picture of interfaces on nanostructured catalytic systems. This was demonstrated for Pt nanoparticles supported on iron oxide thin films which undergo encapsulation by supporting oxide as a result of strong metal/support interaction (see Figure).